Reports

Droplet Impacts Upon Liquid Surfaces

Abstract. *The absorption and rebounding of single droplets and streams of droplets (of diameter less than 1200 micrometers) impacting upon the surface of a deep liquid have been examined experimentally. Conservation of mechanical energy and momentum have been used to explain rebounding droplet interactions, and impaction criteria have been established regarding the absorption of droplet streams. Surface tension is the dominant mechanism governing the observed behavior. Single droplets were never observed to rebound.*

The impaction of droplets upon liquid surfaces is a commonplace but little understood interaction. We report here on an investigation of the collisions of water droplets (of diameter <1200 μm) with water surfaces for an approximately semi-infinite pool. In particular, we attempted to determine the conditions under which the droplets either rebound from, or are absorbed by, the liquid surface. Two different types of incident droplets are used: (i) single droplets (which were never observed to rebound) and (ii) streams of droplets (which were observed to rebound only under certain conditions). The impaction process has been photographed, and the geometry of the surface disturbance is used to relate the energy of the incident droplet to that of the rebounding droplet. The postimpaction behavior of the droplet is also examined, and criteria for the transition from rebounding to absorbing impacts are developed.

Using droplets of diameter >4 mm and vertical velocities >700 cm/sec, Worthington (*1*) examined the splash of a water droplet in a deep pool of water. His observations of a liquid crater and crown formation were quantified by Engel (*2*) for normal impacts in terms of the energy budget of the surface disturbance. Engel's analytical technique is used in the work reported here. Jayaratne and Mason (*3*) investigated the absorption and coalescence of droplets of diameters <1000 μm. They allowed streams of droplets to impinge upon water surfaces and found that the transition between rebounding and absorption was dependent upon the droplet diameter, velocity, angle of incidence, and electrical charge. However, their results are restricted to cases of shallow, horizontally bounded pools and are of limited relevance to the work reported here. They also proposed an interaction model using a layer of air between the droplet and the liquid surface. Other studies (*4–10*) are restricted to the absorbing impacts of primarily large droplets and are of minor importance to this work.

In the experiments, stable streams of uniformly sized, equidistant droplets were formed by transverse modulation of a water stream (*11*). The droplets were initially moving horizontally. They then fell vertically onto the surface of a deep water tank. We controlled the angle of impact by adjusting the droplet fall height. A mechanized shutter was used to interrupt the droplet stream in order to permit a selected number of droplets to strike the surface. The various stages of the collisions were recorded with a microscope-camera and timed stroboscopic illumination. The apogee of the rebounding droplet's trajectory was recorded by a pendulum coated with carbon black located to appropriately intersect the rebounding droplet stream.

In each test the independent variables are the droplet mass (assumed to be constant) and the initial horizontal velocity and elevation. Conservation of momentum and energy permits calculation of a droplet's momentum and kinetic energy upon impact. Similarly, the rebounding droplet's energy and momentum are calculated from the trajectory. The results of the measurements are summarized in Table 1.

Rebounding droplets in droplet streams generally lose different amounts of momentum and energy, and so each

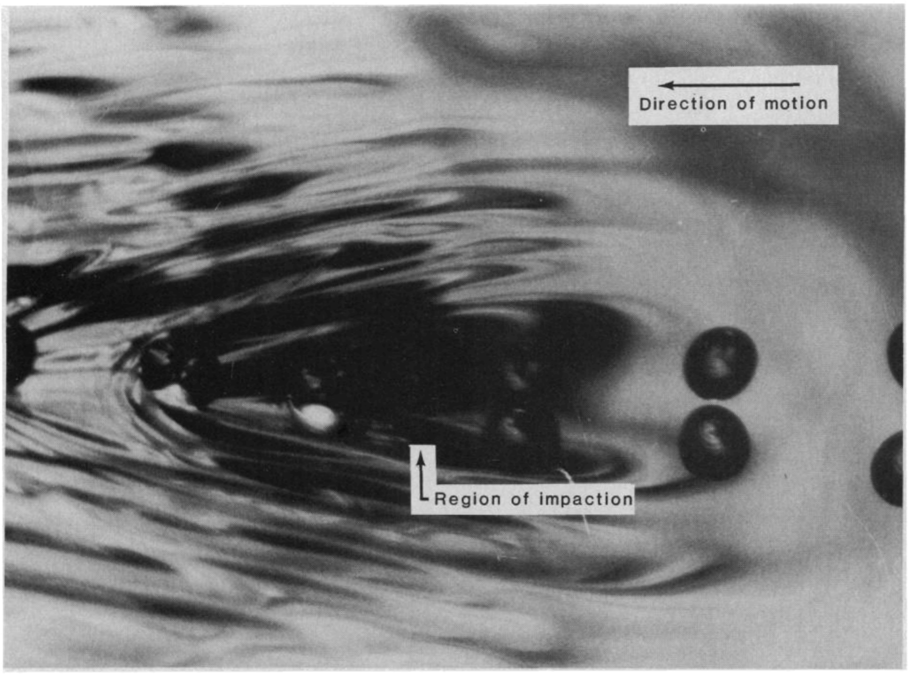

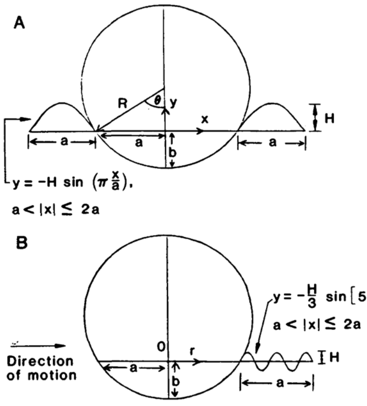

Fig. 1 (left). Multiple resonant rebounding droplet impactions on a liquid surface. Droplet motion is from right to left. The photograph shows an oblique view from above. Fig. 2 (right). Idealized crater and wave formation caused by droplet impaction on a liquid surface. (A) Vertical cross section in the plane normal to droplet motion. (B) Vertical cross section in the plane parallel to droplet motion.

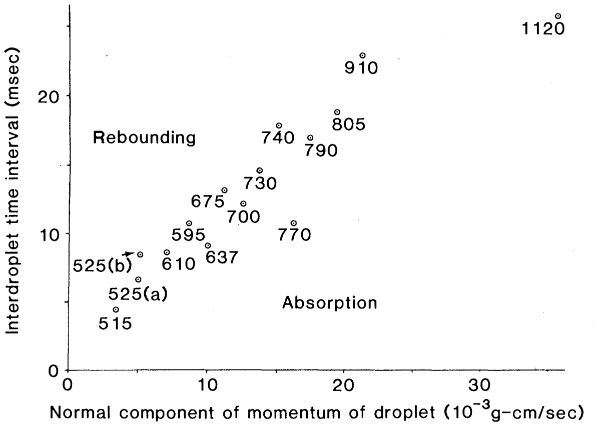

Fig. 3. Droplet rebounding-absorption interface: interdroplet time interval as a function of the normal component of momentum of the droplet in a stream. The droplet diameter (in micrometers) is shown next to each point plotted.

rebounding droplet has a unique trajectory. However, at certain normal velocities a resonant system is established in which all the droplets rebound with the same trajectory. In resonant rebound situations a periodically oscillating crater is formed in the target liquid at the impaction site (Fig. 1). The droplet is decelerated, and some of its energy and momentum are transferred to a horseshoe-shaped wave created by the droplet's motion. The sides of the wave spread laterally as the droplet advances, while the front of the wave moves with the droplet. From observations of the wave geometry one may calculate independently the gravitational, kinetic, and surface tension energy components of the total wave energy and the vertical force acting upon the droplet due to the hydrostatic pressure and surface tension of the target liquid. The quantities measured are the wave and crater amplitudes, lengths, and widths, respectively.

In analyzing the resonant rebounding interaction, the droplet is assumed to create a channel or crater as it moves along the surface. The crater has a long wave on either side and three smaller waves at the front which curve around and join the lateral waves (Fig. 2). There is no wave at the rear of the crater. The amplitude of the frontal waves is assumed (based upon observations) to be one third that of the lateral waves. Both amplitudes are calculated by equating the volume of the crater to that of the waves. One can calculate the total gravitational energy of the wave, which also can be shown to be equal to the total kinetic energy of the wave (*12*), and the surface tension–related increase in the potential energy of the wave-crater system by using the geometrical relationships shown in Fig. 2. The energy budgets of the crater-wave system are summarized in Table 1 for all cases observed. The measurement error is propagated as described by Parrat (*13*) and is typically ±20 percent of the droplet energy loss. By far, most of the energy of the crater-wave system is the portion due to surface tension, and the calculated energy of this system (within the band of measurement error) is equal to that lost by the droplet during the collision.

The vertical momentum change and average force, *F*, upon the droplet during its descent to maximum crater depth may be determined from the equation

$$F = 2\pi\rho g \int_0^a [(R^2 - r^2) + (b - r)^2 + 2(R^2 - r^2)^{1/2}(b - R)]^{1/2} r\,dr + \frac{2\pi\alpha a^2}{R}\sin\theta - mg \qquad (1)$$

where the successive terms arise from the liquid hydrostatic pressure, surface tension, and droplet weight, respectively (ρ is the density of the liquid, g is the gravitational acceleration, m is the mass of the droplet, and α is the surface tension of water). The measured rate of change of droplet momentum and the forces acting on the droplet are displayed in Table 1. By far, the strongest force is that due to surface tension. The best agreement with the measured droplet momentum change is found when the interfacial force is multiplied by a factor, *K*, of 0.75 which is justified because (i)

Table 1. Incident and rebounding measured velocities, energies, and rates of momentum change of the resonant droplet stream.

Droplet diameter (μm)	Incident droplet velocity (cm/sec)		Rebounding droplet velocity (cm/sec)		Calculated kinetic plus gravity energy of site (ergs)	Calculated surface–tension energy of site (ergs)	Calculated total energy of site (ergs)	Measured energy lost by droplet (ergs)	Calculated hydrostatic plus gravity forces (dynes)	Calculated surface–tension force (dynes)	Calculated reduced total force (0.75 *F*) (dynes)	Measured rate of droplet momentum change (dynes)
	Vertical component	Horizontal component	Vertical component	Horizontal component								
525(a)	−19.81	157.5	−17.16	100.1	0.001	0.576	0.577	0.564 ±0.100	−0.078	3.78	2.78	3.16 ±0.10
525(b)	−28.71	100.6	−25.83	70.27	0.000	0.224	0.224	0.202 ±0.044	−0.078	3.78	2.78	3.03 ±0.30
595	−24.66	111.3	−19.31	76.21	0.000	0.351	0.351	0.376 ±0.075	−0.112	3.65	2.66	2.08 ±0.19
700	−22.15	113.4	−17.16	85.78	0.001	0.441	0.442	0.512 ±0.107	−0.181	3.47	2.47	2.26 ±0.17
770	−31.32	181.3	−27.31	163.5	0.003	0.806	0.809	0.763 ±0.098	−0.246	5.71	4.12	7.25 ±0.51
805	−34.02	225.5	−29.05	222.9	0.005	1.994	1.999	2.172 ±0.646	−0.280	5.64	4.04	4.23 ±0.28
910	−26.21	108.6	−21.24	80.82	0.002	0.923	0.925	1.084 ±0.165	−0.401	5.46	3.81	4.41 ±0.27
1120	−28.01	105.0	−25.06	82.22	0.007	1.723	1.730	1.627 ±0.294	−0.752	7.43	5.06	6.26 ±0.31

Eq. 1 averages the force over space only, not time, and the droplet spends more time in the lower half of the crater, where both the hydrostatic pressure and the surface tension force are greater (thereby suggesting that $0.5 \leq K < 1.0$), and (ii) the submerged portion of each droplet (depicted in Fig. 2) is not completely surrounded by water. These successful mechanical analyses have made no use of the air layer hypothesis of Jayaratne and Mason (3).

As the normal incident momentum of a rebounding droplet stream is increased, eventually a point is reached above which no rebounds are observed. The threshold conditions for transition from rebounding to absorption were measured for various droplet sizes, and the results show that the incident normal components of momentum and energy increase with increasing droplet mass. In addition, the interdrop time interval increases monotonically with the incident normal component of momentum (Fig. 3). The explanation of these data remains unclear; however, they are reproducible and consistent and indicate the interface conditions between the two regimes of behavior.

Within the range of incident velocities and droplet diameters examined, single droplets were never observed to rebound. In each single droplet test the droplet control shutter allowed typically four droplets to pass through, and the leading droplet (taken as a single droplet) and all succeeding droplets were always absorbed. Droplet impaction photographs indicate large deceleration of the leading droplet in forming a crater so that this energy loss is sufficient to prevent the droplet from rebounding. Succeeding droplets, however, encounter a partially formed crater and thus must perform less work in the process of crater formation. The shaping of the crater continues, with each droplet losing all of its kinetic energy upon absorption. Finally, an impacting droplet retains enough kinetic energy to escape from the surface, after which all impacting droplets with the same characteristics rebound.

BRUCE CHING
MICHAEL W. GOLAY
THOMAS J. JOHNSON
Department of Nuclear Engineering,
Massachusetts Institute of Technology,
Cambridge 02139

References and Notes

1. A. M. Worthington, *A Study of Splashes* (Longmans, Green, London, 1908).
2. O. G. Engel, *J. Appl. Phys.* **37**, 1798 (1966).
3. O. W. Jayaratne and B. J. Mason, *Proc. R. Soc. London Ser. A* **280**, 545 (1964).
4. F. H. Harlow and J. P. Shannon, *J. Appl. Phys.* **38**, 3855 (1967).
5. P. V. Hobbs and A. J. Kezweeny, *Science* **155**, 1112 (1967).
6. P. V. Hobbs and T. Osheroff, *ibid.* **158**, 1184 (1967).
7. W. C. Macklin and P. V. Hobbs, *ibid.* **166**, 107 (1969).
8. P. R. Brazier-Smith, S. G. Jennings, J. Lantham, *Proc. R. Soc. London Ser. A* **326**, 393 (1972).
9. W. C. Macklin and G. J. Metaxas, *J. Appl. Phys.* **47**, 3963 (1976).
10. S. G. Jennings, *Phys. Educ.* **12**, 381 (September 1977).
11. R. M. Schotland, *Discuss. Faraday Soc.* **30**, 72 (1960).
12. C. A. Coulson, *Waves* (Oliver and Boyd, New York, 1955).
13. L. G. Parrat, *Probability and Experimental Errors in Science: An Elementary Survey* (Dover, New York, 1971).
14. We recognize the essential technical aid provided by the Stroboscopic Light Laboratory staff of H. E. Edgerton. This work was supported, in part, by the U.S. Department of Energy.

23 January 1984; accepted 24 August 1984

Leaf Herbivores Decrease Fitness of a Tropical Plant

Abstract. *Damage by insect herbivores to neighboring individuals of the shrub* Piper arieianum *in a neotropical wet forest varies greatly. This differential damage has a genetic basis and results in a 2-year decrease in growth, seed production, and seed viability, with larger plants recovering before smaller plants. The results provide evidence that leaf herbivores represent a potentially strong selective force for the evolution of plant defenses.*

Theoretical considerations of herbivore-plant interactions assume that the numerous mechanical and chemical characteristics of plants that decrease herbivore feeding, growth, and survival have evolved as a direct result of selection imposed by herbivores (1, 2). However, our understanding of the effects of leaf herbivores in plant evolution is either derived from agricultural systems or correlational evidence of herbivore-caused reductions in plant growth or survival in nature (3, 4). Realistic experiments are scarce (5). Studies of natural populations of the neotropical understory shrub *Piper arieianum* C.DC. (Piperaceae) show a link between intraspecific variation in leaf damage and differential reduction of plant fitness. Naturally high variation in herbivore damage between individual plants and clones appears to be related to substantial long-term effects of simulated herbivore damage on growth, seed output, and associated characters.

Piper arieianum is a common understory shrub at the La Selva Biological Station which is located in lowland tropical wet forest in northeastern Costa Rica (6). Loss of leaf area to herbivores in this species varies greatly between neighboring plants. For individual plants over short time periods (2 to 3 months), leaf area loss attributable to herbivores other than leaf-cutting ants is low, but variance is very high: for nine census periods, the mean percentage of damage and standard deviation ranged from 1.04 ± 1.14 to 6.63 ± 15.31 percent ($n = 25$ plants; extremes in individual plant damage, 0.00 to 25.95 percent) (7). Because leaves live for 1.5 to 2.5 years these relatively small losses over short time periods can sum to large amounts of damage observable at any one time. Single measurements of herbivore damage to entire plants range from 3.93 to 49.65 percent (mean ± standard deviation, 16.74 ± 8.84 percent; $n = 25$ individuals) (8). Statistically significant differences in herbivory between clones of *P. arieianum* strongly suggest that plant genotype differences influence this intraspecific variation in herbivory (9).

To relate intraspecific variation in herbivory to possible differences in plant fitness in *P. arieianum*, I defoliated plants in late November 1980, 2 months before the main flowering peak of the species (10). I used a paper punch to damage leaves for 18 days (11). Within a plant, most leaves receive little natural damage, and a few sustain heavy damage. I simulated these naturally uneven patterns of herbivory by removing small amounts of leaf area from most leaves and heavily damaging the remaining few leaves. The total area removed was 0, 10, 30, or 50 percent of the plant's total leaf area (12). To control for influences of plant size on the effects of defoliation, I classified plants into three size categories (small, medium, or large) at the beginning of the experiment (13) and randomly assigned individuals within each size category to a defoliation level (14). In addition, I completely defoliated 30 medium-sized plants over 1 day by clipping the blade from the midrib of the leaf and removing the cut material from the vicinity of the plant; this simulated damage by leaf-cutting ants.

Growth during the first year after defoliation showed a statistically significant reduction ($P < 0.05$) in small- and medium-sized plants from which 30 percent or more of the leaf area was removed (Fig. 1A) (15). For the full 2 years after defoliation, small- and medium-sized plants with ≥ 30 percent defoliation